Available online at www.sciencedirect.com
SCIENCE DIRECT®
Catalysis Today 98 (2004) 193–199
CATALYSIS TODAY
www.elsevier.com/locate/cattod

Preparation, characterization and evaluation of Maya crude hydroprocessing catalysts

S.K. Maity*, J. Ancheyta, F. Alonso, Mohan S. Rana

Instituto Mexicano del Petróleo, Eje Central Lázaro Cárdenas 152, Col. San Bartolo Atepehuacan, México D. F., 07730, Mexico

Abstract

Two supports, one prepared in our laboratory and other supplied commercially, were used to prepare CoMo and NiMo catalysts. A commercial catalyst was also used as a reference in our present investigation. These catalysts were characterized by XRD and TPR experiments. HDM, HDS, HDN and HDAsp reactions were carried out in a microreactor using a mixture of Maya crude with naphtha as feed. The deactivation of catalysts was also studied. XRD results revealed that the active metals were well dispersed into the supports. Two broad peaks were observed on promoted catalysts in our TPR experiment. Lower temperature peak was assigned as reduction of multilayer MoO_3 species and higher temperature peak was due to reduction of monolayer MoO_3 species. The reduction peak patterns were different for respective catalysts. The catalyst deactivation was observed with time on the stream and it was faster at initial period of reaction. The coke formation was prime concerned for the deactivation of these catalysts as well as the decrease of specific surface area. The activities were correlated with the pore structure of the catalyst.

Keywords: Maya crude; XRD; TPR; Hydroprocessing; HDM; HDS; HDN; Deactivation

1. Introduction

Refineries have undergone restructuring and revamping units due to changes of petroleum feeds properties and the demand of more environment friendly products. The increasing demand of lighter products and middle distillates will be continuing in near future and the demand of heavy crudes, at the same time, will be decreased. To meet this demand, a substantial quantity of heavy crudes has to be upgraded [1–4] and hydroprocessing is one of the mostly used processes in this regard. Since heavier crudes contain various types of contaminants, the refining processes are being modified technologically for upgrading of these feeds. However, the technological change cannot only handle with very tighter environmental legislation. Therefore, several efforts are being attempted for making new generation of catalysts which are more active, more selective, long-lived and more thermally stable.

The main problem during hydroprocessing is the deactivation of catalysts. Activity changes rapidly during first few hours of run and then it becomes stable. It is generally practiced in refineries that the catalyst is allowed to deactivate to a certain level and then temperature is increased to increase reaction rate to compensate the loss of activity due to the catalyst deactivation [5]. The principal causes of the catalyst deactivation are deposition of carbonaceous particle (coke) and formation of metal sulfide on the catalyst. Coke is deposited very rapidly within a few hours of run and then it gets a steady-state, whereas deposition of metal sulfide is continued with run of operation [6–9].

To control the coke formation, special attention has to be paid on pore size, pore volume and pore size distribution of the catalysts. The pore not only gives the paths for reactant and products molecules, but also sites for deactivation. The pore diameter of the catalyst is more critical when the size of reactant molecules is bigger. The coke deposition has an adverse effect on the catalyst porosity. The mode of catalyst deactivation depends on pore diameter. For small pore diameter, catalyst deactivation occurs due to pore mouth

* Corresponding author. Tel.: +52 55 9175 8422; fax: +52 55 9175 8429.
E-mail address: skumar@imp.mx (S.K. Maity).

0920-5861/$ – see front matter © 2004 Elsevier B.V. All rights reserved.
doi:10.1016/j.cattod.2004.07.033

plugging, whereas for large pore diameter, it happens due to core poisoning [10,11].

The presence of vanadium and nickel is particular concern because of the poisoning effect of these metals during hydrodesulfurization and cracking of the feeds. The metals are usually distributed between porphyrin and nonpophyrin type of structures [12–14]. These metal containing compounds are deposited into the catalyst during hydrotreating. Because of their large size, they do not penetrate deeply into the catalyst. These are accumulated as metal sulfides into the pore mouth of the catalyst and block the way to enter the reactants and this causes the deactivation of catalyst [15].

Several efforts have been made to find out the optimum pore diameter to control the deactivation rate [16–19]. It was found that this optimum pore diameter mainly depends on the feed properties. In the present investigation we use four different catalysts for hydrotreating of Maya heavy crude and we try to correlate hydrotreating reactions with the catalyst properties.

2. Experimental

2.1. Preparation of support

Alumina support for this investigation was prepared by pH swing method. Aqueous solutions of sodium aluminum oxide and aluminum sulfate were prepared. Sufficient amount of distilled water was taken into three mouths reactor vessel and heated at 95 °C. First, aluminum sulfate (acid) solution was added into the reactor vessel and heated with continuous stirring. The reaction mixture was allowed for 3 min. Then an equal amount of sodium aluminum oxide (basic) solution was added into vessel and allowed 3 min. The pH of the solution was varied from 4 to 9.5 by adding acid and basic solutions of aluminum salts subsequently. The slurry was allowed 3 min in between the addition of acid and basic solutions. The addition of acid and basic solutions was repeated eight times in total. Finally the solution was aged for 10 min at pH of 9.5. The slurry was then filtered and washed. The cake was formed extrudate having diameter of 1 mm. The extrudate was dried at 100 °C for 7 h and then calcined at 500 °C for 3 h.

2.2. Preparation of catalysts

Catalysts were prepared by sequential incipient wetness technique. An appropriate amount of ammonium heptamolybdate (AHM, Aldrich) salt was dissolved into distilled water. The solution was impregnated on the dry support and the impregnated samples were allowed overnight at room temperature and then dried 7 h at 120 °C and calcined at 450 °C for 3 h. Cobalt/nickel promoter was also impregnated over the Mo loaded catalysts and dried and calcined as similar procedure as mentioned above. Cobalt nitrate (or nickel nitrate) (Baker) was used for this impregnation. Catalysts A and B were prepared by laboratory made gamma alumina (AS) and catalyst C was prepared by commercial gamma alumina (AC, Condea). Catalyst A contains 10 wt.% of MoO_3 and 3 wt.% of CoO as catalyst basis. Both catalysts B and C contain 10 wt.% of MoO_3 and 3 wt.% of NiO. The reference catalyst (D) consists of 10.66 wt.% of MoO_3, 2.88 wt.% of NiO and 3.73 wt.% of TiO_2 and it is supported by gamma alumina.

2.3. Catalyst characterization

X-ray diffractograms were recorded on a SIEMENS D-500 model using a Cu Kα radiation. Temperature programmed reduction (TPR) apparatus consisted of a quartz reactor and a thermal conductivity detector (TCD). Heating was performed with tubular furnace regulated by a temperature controller. The reducing gas consisted of a mixture of 10% H_2 in argon. The reducing gas mixture was purified by molecular sieves. For each TPR experiment, 0.1 g of catalyst weight was taken. Before each run, the baseline was stabilized at room temperature by passing gas mixture at a flow rate of 25 ml/min. After stabilization the sample was heated at 10 °C/min from room temperature to 1200 °C.

BET specific surface area (SA), pore volume (TPV) and pore size distribution (PSD) of fresh and spent catalysts were measured by nitrogen adsorption at 77 K (Automatic Micromeritics ASAP2100). The percentage of carbon and metals was also measured on spent catalysts. The spent catalysts were washed with hot toluene by Soxhlet process and dried at 110 °C before carbon and metal analyses. The coke is defined in this work as being carbon content on spent catalysts.

Total metals (ASTM D-5863) in the feed and products were measured by atomic absorption. Sulfur (ASTM D-4294) and nitrogen were analyzed by X-ray fluorescence and chemiluminescence, respectively. Asphaltene was the insoluble fraction in *n*-pentane (ASTM D-2007).

2.4. Presulfiding of catalyst

The oxide catalyst was sulfided in situ before actual run was started. About 10 ml of oxide catalyst was loaded with an equal volume of diluent, carborandum. The size of carborandum is 0.2 mm. Both the catalyst and carborandum were mixed and divided into five parts. Each part of the mixture was loaded into the reactor at a time and trapped a little bit. The catalyst was then dried for 2 h at atmospheric pressure at 120 °C. After drying, catalyst was allowed to soak for 2 h at 150 °C and light gas oil (LGO) was used for soaking. This light gas oil contains 1.7 wt.% of sulfur. Actual sulfiding agent was introduced after soaking. Sulfiding agent was a mixture of LGO with dimethyl disulfide (DMDS, 1 wt.%). Sulfidation was done at 28 kg/cm^2 pressure at two different temperatures. First sulfidation was done at 260 °C for 3 h and finally it was done at 320 °C for 5 h.

2.5. Catalyst activity test

Catalyst activity tests were performed in a high pressure fixed-bed microreactor in up flow mode. Description of this unit and the experimental procedure were given elsewhere [20]. The experimental conditions are: total pressure, 54 kg/cm^2; reaction temperature, 380 °C; liquid hourly space velocity (LHSV), 1.0 h^{-1}; hydrogen-to-hydrocarbon ratio, 356 m^3/m^3. A mixture of Maya heavy oil with hydrodesulfurized naphtha (50/50 wt./wt.) was used for catalyst activity tests. The hydrodesulfurized naptha is used as a diluent since our plant is not capable to handle 100% Maya heavy crude.

3. Results and discussion

3.1. Properties of feed and catalysts

In our present investigation we used a mixture of Maya heavy crude with hydrodesulfurized naphtha (50/50 wt./wt.) as a hydrotreating feed for catalyst activity test. Nickel, vanadium, sulfur, nitrogen and asphaltene contents of the feed are 26.17, 123.35 wppm, 1.856, 0.253, and 7.96 wt.%, respectively.

Physical properties of the laboratory made support (AS) and Condea supplied support (AC) were measured by nitrogen adsorption and the results are given in Table 1. Physical properties of fresh and spent catalysts are also given in the same table. Physical properties of spent catalysts were measured after washing them with hot toluene and subsequent drying. The pore size distribution of the fresh and spent catalysts is also presented in Fig. 1. Figure shows that the laboratory prepared support is bimodal in nature. Total pore volume and average pore diameter (APD) of support, AC are higher than these for support AS.

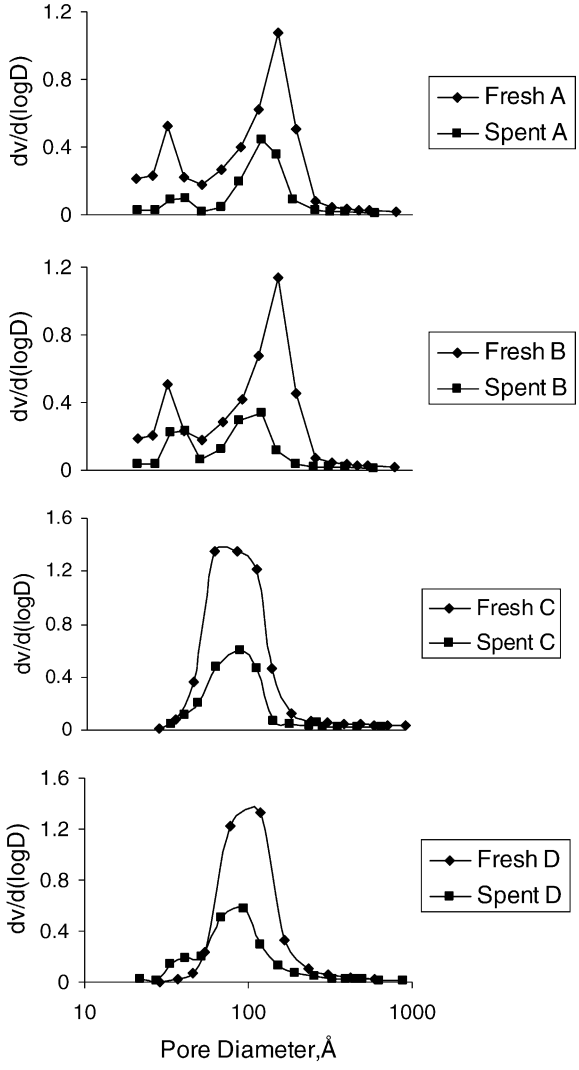

Fig. 1. Pore size distribution of fresh and spent catalysts.

3.2. X-ray diffraction (XRD)

X-ray diffractograms of pure support (AS) and of catalysts A, B, C are given in Fig. 2. It clearly shows that the support used in this investigation is gamma alumina. No additional peaks are observed with the addition of molybdenum on the support. This indicates that molybdenum atoms are well dispersed on alumina support. It is also observed that the XRD peaks intensity decreases with the addition of metals atom and it is more prominent in cobalt

Table 1
Physical properties of supports, fresh and spent catalysts

Properties	Supports		Catalysts							
	AS	AC	CoMo/AS (A)		NiMo/AS (B)		NiMo/AC (C)		Reference (D)	
			Fresh	Spent	Fresh	Spent	Fresh	Spent	Fresh	Spent
SA (m^2/g)	302	240	262	136	257	148	223	191	156	147
TPV (cc/g)	0.574	0.763	0.496	0.154	0.489	0.169	0.645	0.344	0.55	0.258
APD (Å)	76	124	73	40	74	50	114	52	142	68
PSD (vol %)										
>1000 Å	1.8	–	–	–	–	–	0.69	–	–	–
1000–500 Å	26.37	2.08	1.52	2.45	1.74	2.37	1.73	2.40	1.97	2.16
500–200 Å	41.48	4.87	14.32	10.39	12.4	4.98	4.93	4.55	8.9	6.47
200–100 Å	13.82	43.94	45.30	60.21	47.58	40.85	41.63	18.69	57.7	35.41
100–50 Å	5.75	46.58	15.30	12.82	15.94	23.98	48.00	33.36	30.68	42.98
<50 Å	10.78	2.53	23.56	14.17	22.34	27.82	3.02	41.0	0.75	12.98

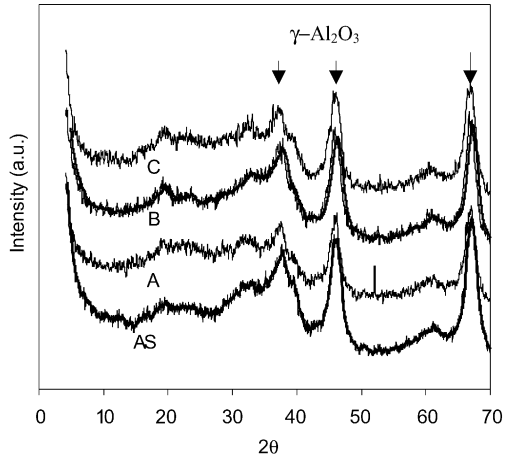

Fig. 2. XRD diagrams of pure alumina and supported catalysts.

promoted catalyst (A) indicating that molybdenum is strongly bonded with the alumina support and hence more molybdenum dispersed phases are expected to be present.

3.3. Temperature programmed reduction (TPR)

The TPR profiles of pure alumina and alumina supported catalysts are presented in Fig. 3. Pure alumina, which is prepared in our laboratory, shows high temperature reduction peak. The reduction peak is broad in nature and the maximum reduction temperature (T_m) appears at 674 °C. The molybdenum loaded catalyst on this support shows very sharp reduction peak at 516 °C. We do not observe any reduction corresponding to pure alumina in this catalyst.

The TPR profiles are completely changed with the addition of promoters (Co or Ni) into the Mo loaded catalyst. Two very broad peaks are observed for both Co and Ni promoted catalysts. These broad and highly complex bands

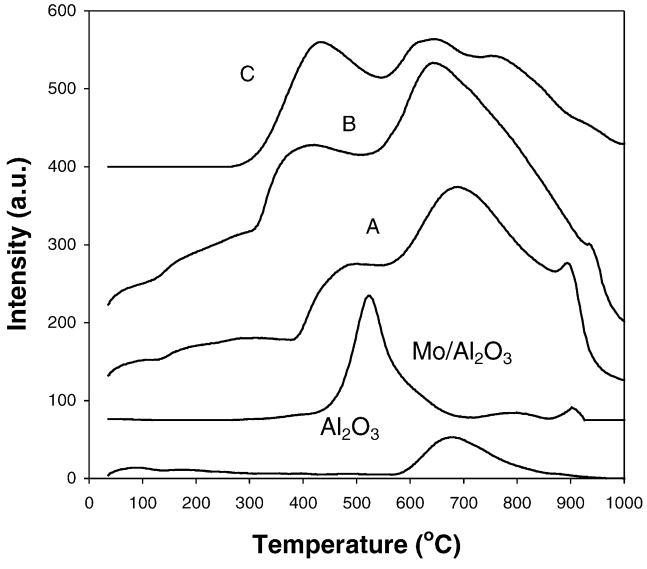

Fig. 3. TPR patterns of pure alumina and supported catalysts.

may be composed of the superposition of various peaks. One peak is observed at lower temperature and another one is found at higher temperature compared with the reduction peak of Mo/Al_2O_3 catalyst. It is also seen that total peak area increases drastically. It indicates that the more reducible species are present on promoted catalysts than unpromoted one. If we compare the reduction behavior of NiMo and CoMo catalysts, we observe that both high and low temperature reduction peaks appear at lower temperature in NiMo catalyst.

The TPR profile of (C) in Fig. 3 corresponds to the reduction pattern of NiMo supported on commercial support (AC). This TPR pattern is different from the others, since three broad reduction peaks are present. Both supports AS and AC are gamma alumina but their preparation procedures are different. When metals are impregnated into the support and calcined subsequently, metal atoms interact with the basic hydroxyl groups of support and a new bond is formed between metal and support through O atom as illustrated below:

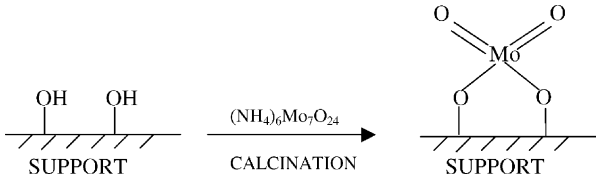

The nature of the hydroxyl groups is different for different aluminas, which are prepared by different methods. Hence it is expected that the nature of bonding between metal and support is also different for different supports. That may be the reason to show different reduction patterns for catalysts supported on AS and AC.

The reduction peak for pure alumina appears at 674 °C. In promoted catalysts, higher temperature reduction peak is observed in 650–685 °C temperature range. This peak does not correspond to reduction of pure alumina. If so, we should also observe this peak on Mo/AS catalyst. However, we do not observe. Therefore, we can say that this higher temperature peak is not due to reduction of pure alumina but due to reduction of strongly bonded monolayer of MoO_3. The lower T_m, which is broader than the higher T_m, is presumably attributed to reduction of Mo multilayers.

One can also explain the nature of two broad peaks of promoted catalysts in the following way. Mo/AS catalyst shows one reduction peak, and Co or Ni promoted catalysts show two broad reduction peaks. It may be said that one peak is due to reduction of MoO_3 species and the other one may be due to reduction of CoO or NiO type of species. But it is not true if we look work done by others in this direction. Brito and Laine [21] observed two reduction peaks on Mo/Al_2O_3 catalyst. With the addition of Ni into Mo loaded catalyst, they found very small satellite in between two peaks at 3 wt.% NiO loading. The intensity of this satellite increases with the increase of NiO content. But the overall intensity of the satellite is very weak compared with broad

peaks corresponding to reduction of MoO_3. In our case, both reduction peaks are very high in intensity. Therefore, it advocates that another reduction peak is not attributed to the reduction of NiO or CoO species.

The ratio of peak area of low T_m to high T_m is higher in NiMo catalyst compared with CoMo catalyst. It means that the presence of multilayer MoO_3 is more in NiMo catalyst. The interaction between MoO_3 phases with support in NiMo catalyst is also weaker, since we observe T_m shift to lower temperature. The similar conclusion was also drawn by Brito and Laine [21]. We also observed the stronger interaction between metal and support in CoMo catalyst compared with NiMo catalyst from our XRD experiments.

3.4. Activities study

The hydrodemetallation (HDM), hydrodesulfurization (HDS), hydrodenitrogenation (HDN) and asphaltene conversion (HDAsp) are studied using a mixture of Maya heavy oil with naphtha. Initial activities of these four catalysts are given in Fig. 4. The HDM activity of catalyst C is the highest of all four catalysts. The catalyst D, which is taken as a reference in this study, shows lower HDM activity than catalysts C and A.

Average pore diameter (APD) of the catalyst D is the biggest of all four catalysts studied. APD of catalysts A and B are the same, because these two catalysts were prepared using the same AS support. APD of catalyst C is higher than those of catalysts A and B but it is smaller than catalyst D. It is known that metal compounds in the heavy oils are very big complex molecules and removal of these metal compounds from crude is a diffusion limited reaction. APD of catalyst C is considerably big and that may be the reason for showing higher HDM activity. However, catalyst D shows less HDM activity than catalyst C though APD of the former is bigger than the latter. Therefore, our results do not satisfy the diffusional restriction. It should be noted that the HDM activities of all catalyst are closed to each other and therefore it is difficult to give an explanation only with respect to pore size. Moreover, our asphaltene conversion results also support the above conclusion. Asphaltene molecules are also very big in size and it is well documented to be diffusional restricted reaction. Hence, catalyst C should show higher HDAsp activity compared with the other two catalysts. However, we obtain reverse result, i.e., catalyst C shows less HDAsp conversion.

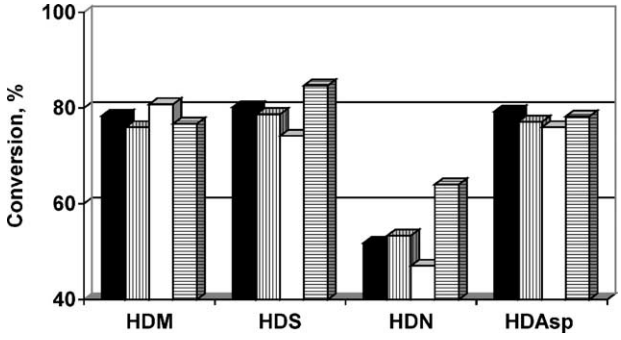

Fig. 4. Percentage of initial conversions of four catalysts (■ A, ▥ B, □ C, and ▤ D).

Catalyst A shows higher HDM activity than catalyst B. These catalysts are prepared using the same the support, AS. The difference is that the former is promoted by Co and the latter is promoted by Ni. Therefore, we can say that Co promoted catalyst is better than Ni promoted catalyst in respect of HDM activity when other parameters, support and active metal, are the same for both cases. Other possible explanation of higher HDM activity of catalyst A is the presence of more reducible MoO_3 species as observed from TPR experiment.

HDS and HDN activities of the catalyst D are the highest. HDS and HDN activities of catalyst C are lower than the other two catalysts. The specific surface area of the support of catalyst C is less and that may be the reason for showing less activities compared with the other two catalysts. Although specific area of catalyst D is very low compared with the other catalysts, it gives the highest HDS and HDN activities. The presence of titania into this catalyst is the reason to show higher activities.

Both HDS and HDN conversions slightly decrease with the increase of APD and then these increase with further increase of pore size. It indicates that the average pore diameter for all the catalysts studied here is sufficiently large to enter the reactants and therefore, no diffusional restriction is observed. However, the highest HDS and HDN activities of the catalyst D having large pore diameter is already mentioned above and that is the presence of titania.

3.5. Deactivation study

Metals, carbon, sulfur and nitrogen contents in the deactivated catalysts are given in Table 2. It is observed from this table that there is considerable coke deposition into the catalysts within 64 h of operation. Among four catalysts, coke deposition is maximum on catalyst C and it is 18 wt.% of catalyst. Sulfur deposition is the highest on the reference catalyst D and it is lowest on catalyst A. Iron deposition is almost the same on all the spent catalysts. The maximum amount of V is deposited on catalyst D.

Specific surface area, total pore volume, average pore diameter and pore size distribution of fresh catalysts are

Table 2
Weight percentage of C, S, N and metals on spent catalysts

Catalysts	A	B	C	D
C (carbon)	15.38	16.7	18.02	13.21
S	2.16	3.0	3.1	4.22
N	0.5	0.6	0.6	0.48
Fe	0.03	0.03	0.02	0.04
V	0.69	0.63	0.67	1.11

totally changed in corresponding spent catalysts (Table 1). The changes in pore size distribution are clearly seen from Fig. 1. Decreases of specific surface area, total pore volume and average pore diameter are observed in spent catalysts compared with fresh ones which are mainly due to coke and metals deposition. Maximum specific surface area is lost in catalyst A whereas it is very minimum in catalyst D. Losses of 50–69% of total pore volume are observed in all spent catalysts. More than 50% of average pore diameter is also decreased in catalyst C. Table 1 shows that loss of specific area of catalyst D is very little whereas it is high in other catalysts. This table also shows that the catalysts having large amount of small pores (A and B) lead to higher losses of surface area and pore volume, and it is due to plugging of pore volume. In the catalyst having larger pores, coke or metal sulfide can penetrate into the catalyst pellet and hence the reduction of surface area and pore volume are less.

Activities of all four reactions were studied with respect to time-on-stream as presented in Fig. 5. This figure shows

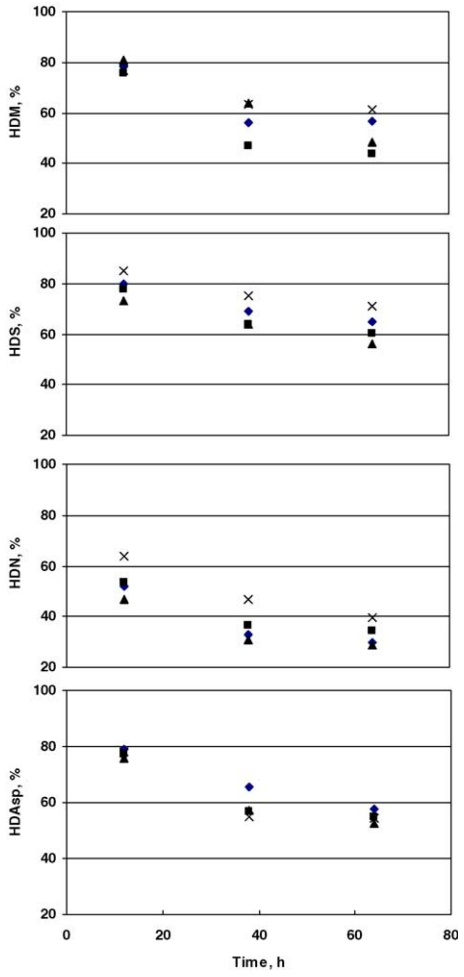

Fig. 5. Percentage of conversions with hours of operation (◆ A, ■ B, ▲ C, × D).

that HDM activity of catalyst C decreases rapidly with run of operation. HDM activity is decreased by 42% after 64 h of run. In this respect catalyst D is more stable compared with all catalysts. The deactivation trends for asphaltene conversion are almost similar for all four catalysts.

The HDS activity of catalyst D decreases 17% in 64 h whereas it is 23% in the case of catalyst C. Deactivations of catalysts A and B are in between catalysts C and D. In the case of HDN, deactivation trends are observed for all four catalysts.

To look more insight on deactivation tendency, a correlation was made according to the following equation [22,23]:

$$X_t = X_0\, e^{-bt^n}$$

where X_t is the conversion at time t, X_0 the initial conversion, b the deactivation rate constant, $n = 1$ (used according to the Ref. [23]).

$\ln(X_t/X_0)$ is plotted against time of operation for HDM, HDS, HDN and HDAsp reactions in Fig. 6. It is clearly seen from this figure that the rate of deactivation is not the same for all the catalysts and it is also noted that deactivation rates are different for different reactions. Several factors are responsible for the deactivation rate like nature of supports, active metals, feed properties, reactions conditions etc. However, it is clear from figure that the deactivation rate is faster at initial period of reaction and then becomes slower. These happen for all cases, irrespective of the catalyst and type of reaction.

The decrease of activities is mainly due to coke deposition on catalysts. Catalyst is deactivated during hydroprocessing of heavy crude with hours of operation. During hydroprocessing pore mouth of catalysts is blocked by coke or by metals sulfide. From Table 2 we observe that there is a less amount of metal deposited on spent catalysts. However coke percentage on spent catalysts is high. Hence in our case the main cause of deactivation is coke. We have also observed similar fact in our other studies [24–26]. It was discussed earlier that primary source of coke is asphaltene content in the feed. The feed used in our present investigation contains high amount of asphaltene. The rapid deactivation for all four reactions is observed on catalyst C. It is also seen that the coke formation on this catalyst is high, indicating that deactivation of the catalyst is mainly due to coke formation on catalyst surface.

We have mentioned that the catalyst D showed comparatively more stability with respect of hour of operation. We also reported that coke deposition in this catalyst is less compared with other three catalysts. As observed from Table 1 and Fig. 1, pore size distribution is changed in spent catalysts compared with fresh ones. The percentage of pore volume below 200 Å region increases in spent catalysts. As substantial increased of pore volume in this region is observed in spent catalyst D, it may be the reason for this catalyst to sustain stability with run of length.

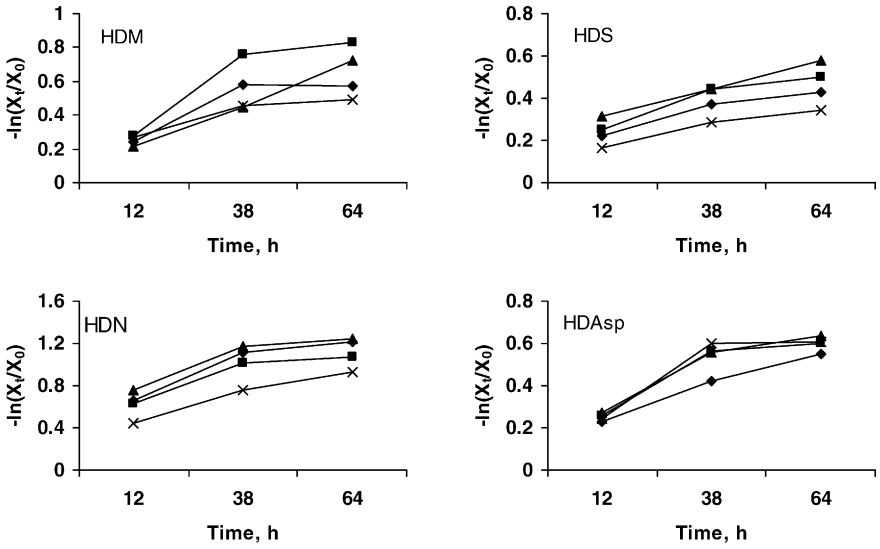

Fig. 6. Data fit for modified Voorhies deactivation correlation (◆ A, ■ B, ▲ C, × D).

4. Conclusions

In our present investigation, pH swing method is used for preparation of support and in this method bimodal type of support is obtained. The TPR experiment shows that metal-support interaction is different for different catalyst though similar type of support, gamma alumina, is used for catalyst preparation. The TPR results also show that more dispersed phases are present in Co promoted catalyst and this may be the reason for this catalyst to show higher activities compared with Ni promoted catalyst. The deactivation rate is faster at initial period of time of operation and it becomes slower with time-on-stream. The coke deposition on the catalyst surface is the main cause for the catalyst deactivation. The coke tends to deposit on the catalyst having higher specific surface area resulting drastic reduction of specific surface area.

Acknowledgment

The authors would like to thank Instituto Mexicano del Petróleo for the financial support.

References

[1] W.I. Beaton, R.J. Bertolacini, Catal. Rev. Sci. Eng. 33 (3/4) (1991) 281.
[2] R.L. Dickenson, F.E. Biasca, B.L. Schulman, H.E. Jonnson, Hydrocarbon Process. February (1997) 57.
[3] W. Weirauch, IFP forecasts global energy use to reach 11.6 btoe/year in 2010, Hydrocarbon Process. November (1997) 25.
[4] F. Tamburrano, Disposal of heavy oil residues. part 1, Hydrocarbon Process. September (1994) 79.
[5] M. Absi-Halabi, A. Stanislaus, D.L. Trimm, Appl. Catal. 72 (1991) 193.
[6] H. Topsoe, S. Clausen, F.E. Massoth, Hydrotreating Catalysis Science and Technology, Springer-Verlag, 1996.
[7] E. Furimsky, F.E. Massoth, Catal. Today 52 (1999) 381.
[8] F. Morel, S. Kressmann, V. Harlé, S. Kasztelan, Hydrotreating Hydrocracking of Oil Fractions, Elsevier, Amsterdam, 1997.
[9] D.L. Trimm, Catalysts in Petroleum Refining 1989, Elsevier, Amsterdam, 1990.
[10] E. Furimsky, Appl. Catal. A 171 (1998) 177.
[11] R.E. Baltus, Fuel Sci. Technol. Int. 11 (1993) 751.
[12] T. Ohtsuka, Catal. Rev. Sci. Eng. 16 (2) (1977) 291.
[13] R. Agralwal, J. Wel, Ind. Eng. Chem. Process. Des. Dev. 23 (1984) 505.
[14] R. Agralwal, J. Wel, Ind. Eng. Chem. Process. Des. Dev. 23 (1984) 515.
[15] G. Gualda, S. Kasztelan, J. Catal. 161 (1996) 319.
[16] R.J. Quann, R.A. Ware, H. Chi-Wen, J. Wei, Adv. Chem. Eng. 14 (1988) 95.
[17] H.A. Hardin, M. Ternan, R.H. Packwood, CANMET Report 81-4E, Energy, Mines and Resources, Canada, 1981.
[18] M. Shimura, Y. Shiroto, C. Takeuchi, Ind. Eng. Chem. Fundam. 25 (1986) 330.
[19] S. Kobayashi, S. Kushiyama, R. Aizawa, Y. Koinuma, K. Inoue, Y. Shimizu, K. Egi, Ind. Eng. Chem. Res. 26 (1987) 2241.
[20] L.C. Castaneda, F. Alonso, J. Ancheyta, S.K. Maity, E. Rivera, M.N. Matus, Energy Fuels 15 (2001) 1139.
[21] J. Brito, J. Laine, Polyhedron 5 (12) (1986) 179.
[22] A. Voorhies, Ind. Eng. Chem. 37 (1945) 318.
[23] Y.W. Chen, W.C. Hsu, Ind. Eng. Chem. Res. 36 (1997) 2526.
[24] S.K. Maity, J. Ancheyta, L. Soberanis, F. Alonso, M.E. Llanos, Appl. Catal. A 244 (2003) 141.
[25] S.K. Maity, J. Ancheyta, L. Soberanis, F. Alonso, Appl. Catal. A 250 (2003) 231.
[26] S.K. Maity, J. Ancheyta, L. Soberanis, F. Alonso, Appl. Catal. A 253 (2003) 125.